Juno Plasma Wave Observations at Europa

W. S. Kurth[1], D. R. Wilkinson[1], G. B. Hospodarsky[1], O. Santolík[2,3], T. F. Averkamp[1], A. H. Sulaiman[4], J. D. Menietti[1], J. E. P. Connerney[5], F. Allegrini[6,7], B. H. Mauk[8], and S. J. Bolton[6]

[1]Department of Physics and Astronomy, University of Iowa, Iowa City, IA 52242 USA
[2]Department of Space Physics, Institute of Atmospheric Physics of the Czech Academy of Sciences, Prague, Czechia
[3]Faculty of Mathematics and Physics, Charles University, Prague, Czechia
[4]Minnesota Institute for Astrophysics, School of Physics and Astronomy, University of Minnesota, Minnesota, USA
[5]Goddard Space Flight Center, Greenbelt, MD, USA
[6]Southwest Research Institute, San Antonio, TX, USA
[7]Department of Physics and Astronomy, University of Texas at San Antonio, San Antonio, TX, USA
[8]The Johns Hopkins University Applied Physics Laboratory, Laurel, MD, USA

Key Points:

- Two chorus bands, electrostatic solitary waves and upper hybrid emissions are observed at Europa.
- Plasma densities near Europa derived from the upper hybrid resonance frequency peak near the wake axis at about 330 cm^{-3}.
- Micron-sized dust impacts peak near closest approach to Europa.

Corresponding author: W. S. Kurth, william-kurth@uiowa.edu

Abstract

Juno passed by Europa at an altitude of 355 km on 29 September, day 272, 2022. As one of Juno's in situ science instruments, the Waves instrument obtained observations of plasma waves that are essential contributors to Europa's interaction with its environment. Juno observed chorus, a band at the upper hybrid frequency providing the local plasma density, and electrostatic solitary structures in the wake. In addition, impulses due to micron-sized dust impacts on Juno were recorded with a local maximum very close to Europa. The peak electron density near Europa was ~ 330 cm^{-3} while the surrounding magnetospheric density was in the range of 50 to 150 cm^{-3}. There was a significant separation between the Europa flyby and Juno's crossing of Jupiter's magnetic equator, enabling a unique identification of effects associated with the moon as opposed to magnetospheric phenomena normally occurring at the magnetic equator near 10 Jovian radii.

Plain Language Summary

Plasma waves are electromagnetic fields occurring in a plasma due to motions of the charged particles comprising the plasma. These waves can arise at various locations and at a range of frequencies depending on many factors, such as the number density of charged particles and the strength of the magnetic field. Here we discuss plasma waves observed by Juno during its 355-km flyby of Europa on 29 September 2022. Some waves, called upper hybrid resonance emissions can provide information on the plasma density. Other waves, called electrostatic solitary waves are indicative of electron beams in the plasma. And yet other waves, called whistler-mode chorus, are important in the interchange of energy between electrons and the waves, resulting in the acceleration of the electrons. Each of these types of waves were observed near Europa by the Juno plasma wave instrument and they are diagnostic of Europa's interaction with the Jovian magnetosphere. The Waves instrument also detects electrical impulses due to the collision of the spacecraft with dust grains moving at over 23 km/s that allow a determination of the concentration of dust near Europa.

1 Introduction

On 29 September, day 272, 2022, Juno passed by Europa at an altitude of 355 km over the leading hemisphere which is also the downstream hemisphere relative to the corotational flow of magnetospheric plasma past the moon. Europa is the subject of intense interest due to its liquid water ocean (Khurana et al., 1998; Kivelson et al., 2000) and potential for habitability (Pappalardo et al., 2013). The ocean under Europa's icy crust was inferred from the Galileo magnetometer observations (Kivelson et al., 1992) that revealed magnetic induction in an electrically conductive interior (Khurana et al., 1998). Hence, the magnetospheric interaction of this moon with the Jovian magnetosphere is of importance to how the moon relates to its environment. The observations of possible plumes (Roth et al., 2014; Sparks et al., 2017) suggests current geologic activity. Jia, Kivelson, Khurana, & Kurth, 2018 retrospectively examined magnetic field and plasma wave data from the Galileo E12 flyby and used modeling to make a case that Galileo may have observed a plume in situ. Hence, plasma waves play an important role in understanding Europa's magnetospheric interaction. This interaction manifests in an auroral spot in Jupiter's ionosphere (Bonfond et al., 2017; Moirano et al., 2021) as well as a relatively short tail extension in the direction of corotation. This is evidence of an electromagnetic interaction including an Alfvén wing (Volwerk et al., 2007), currents, and electron beams connecting Europa to Jupiter.

Galileo provided the first observations of plasma waves in the vicinity of Europa (Gurnett et al., 1998; Kurth et al., 2001). These observations provided electron densities in the vicinity of Europa via the frequency of the upper hybrid band f_{uh} or the or-

dinary mode cutoff at the electron plasma frequency f_{pe}. Whistler-mode emissions were reported in the vicinity of Europa as well as broadband electrostatic noise.

This paper provides an overview of Juno plasma wave observations near Europa more than 20 years after Galileo's last flyby of the moon (E26). While not delving into any one aspect of Europa's plasma wave environment in de-tail, it provides a bridge to new observations in the next decade by the JUICE (Jupiter Icy Moons Explorer) and Europa Clipper missions.

2 Observations

The geometry of Juno's flyby of Europa is given in Figure 1 in the so-called EPhiO Europa-centered co-rotational coordinates in which X is in the direction of co-rotation, Z is parallel to Jupiter's spin axis, and Y completes the orthogonal system and points in the direction of Jupiter (Joy & Mafi, 2002). The flyby occurred at a Jovicentric magnetic local time of 18.75 h and the System III longitude was 136°. From Figure 1 one can see that closest approach is within the geometric wake and near Europa's equator. Juno is within the geometric wake for approximately 3 minutes from $\sim$ 09:34 to 09:37 UT. During the flyby, Juno moves from south to north and towards Jupiter.

The Juno Waves instrument is described in Kurth et al., 2017. The instrument provides simultaneous and orthogonal detection of one magnetic and one electric component of waves in the range of 50 Hz to 20 kHz. The measured magnetic component is parallel to Juno's spin axis (z-axis) and the electric antenna measures fields parallel to the spacecraft y-axis. The spacecraft x-axis is aligned with the solar panel supporting the magnetometer boom. Hence, the x- and y-axes define the spin plane of Juno. This configuration allows, when there is a sizable component of Jupiter's magnetic field parallel to the spacecraft x-axis, the determination of the sign of the Poynting flux of electromagnetic waves relative to the Jovian field, i.e. parallel or anti-parallel (Mosier & Gurnett, 1971; Kolmašová et al., 2018). Waves also measures the electric field to frequencies as high as 40 MHz.

Figure 2 shows the context of the plasma waves near Europa during the perijove 45 flyby. The plasma wave observations are from the burst mode in which continuous waveforms are simultaneously collected for $\sim$ 122 ms from the search coil magnetometer and electric field antenna from 50 Hz to 20 kHz. These are Fourier transformed on the ground to produce the frequency-time spectrograms in panels d and c, respectively. A spectrum is computed every second in this mode. Panel c shows the electric field from 10 to 150 kHz. Panel a gives the electron density n_e based on the frequency of upper hybrid waves in panel c using $n_e = f_{pe}^2/8980^2 = (f_{uh}^2 - f_{ce}^2)/8980^2$ where f_{uh} is the upper hybrid resonance frequency, f_{ce} is the electron cyclotron frequency ($28|B_0|$ in nT), and f_{pe} is the electron plasma frequency. All frequencies are in Hz and the electron density is in cm^{-3}. The magnetic field B_0 is measured by the Juno magnetometer (Connerney et al., 2017). As a special case of electron cyclotron harmonic emissions, upper hybrid emissions discontinuously jump between bands, hence the plasma frequency derived from these emissions is limited in accuracy by order f_{ce}. Panel a shows that for the region surrounding Europa, the electron density is in the range of $\sim$50 to 150 cm^{-3} but with a significant peak at Europa, discussed below.

The interval shown in Figure 2 is extended earlier in time to include Juno's crossing of the magnetic equator because that is the location of significant wave activity in the Jovian magnetosphere at this radial distance whether Europa is nearby or not. Specifically, strong electron cyclotron waves occur between harmonics of f_{ce} as seen in Figure 2b and whistler-mode chorus is seen above and below $f_{ce}/2$ as evidenced by discrete elements shown in Figure S1a in the Supporting Information. Whistler mode emissions can be seen at even lower frequencies in panels c and d. These emissions are distributed

around the magnetic equator, which was crossed near 08:58 UT. The Europa flyby on the other hand, is at 09:36:29, occurring at a magnetic latitude of about 5.1°. Hence, in the following discussion we are confident that the plasma waves near Europa are specific to the Europa-magnetosphere interaction.

Figure 3 shows an expanded view of plasma waves within about 4 Europa radii (R_E) of the moon. The format of Figure 3 is similar to that in Figure 2 except that we have used a logarithmic frequency axis for the low-frequency panels (c - e) and added panel e to show the ratio of E/cB (c is the speed of light, B is the wave magnetic field and E is the wave electric field), a way of distinguishing between electromagnetic and quasi-electrostatic emissions (c.f. Gurnett & Bhattacharjee, 2017). The expanded time scale allows details of the upper hybrid frequency-time structure, particularly near the peak density $\sim$ 09:35:30 where these emissions appear to step down in regular frequency increments similar in magnitude to f_{ce}. This is a common feature of upper hybrid emissions that are organized by harmonics of f_{ce} and happens when the plasma density, hence f_{pe}, decreases (or increases) with respect to the cyclotron frequency. In fact, these emissions appear weakly at even higher frequencies than the 150 kHz filter roll-off of the Waves low frequency receiver. While not shown in this figure, Figure S2 shows them in detail. The electron densities, shown in Figure 3a are highest within the geometric wake and actually peak shortly before closest approach, near the center of the wake. We caution that the f_{uh} emissions appear sporadically throughout the intervals shown in Figures 2 and 3. There are many possible reasons for this including variations in the local electron distribution and polarization that may render them less visible depending on the spin phase of the electric antenna. See Text S1 and Figure S2 in the Supporting Information.

Perhaps the most prominent feature in Figure 3 is the region marked ESW (electrostatic solitary waves) in panel c, the electric component of waves below 20 kHz. These are barely detectable in the search coil (panel d) and show up prominently in panel e with $E/cB \gg 1$. The vertical dashed lines in Figure 3 show times when the strongest bi-directional field-aligned electron beams are observed by the JADE instrument (McComas et al., 2017) at energies below $\sim$300 eV (Allegrini et al., 2022). Note that these beams coincide with the most prominent ESWs, but the ESWs extend throughout the wake region although some of this low-frequency spectum could include other types of quasi-electrostatic modes as yet unidentified. Example waveforms showing evidence of ESW's are given in Figure S3.

There is a band of chorus beginning just before closest approach and extending for $\sim$ 2 minutes, well beyond the geometric wake. This band exhibits a small E/cB ratio in panel e, indicative of an electromagnetic emission, as expected for chorus. There is some weak and relatively narrowband chorus prior to entering the geometric wake, before about 09:34. After closest approach there are two components of the chorus observed. Figure S4 shows the chorus observations with an expanded, linear frequency scale for more clarity. One of the bands has a broad bandwidth and is centered at lower frequencies, near 3 kHz. The other component is very narrow and lies just below $f_{ce}/2$. Figure S1b in Supporting Information shows discrete structures in these emissions, reinforcing the interpretation of chorus. On close inspection of Figure S4, this component appears to switch from bursty and quasi-electrostatic to a more continuous band with a significantly lower E/cB, suggesting more parallel propagation. Santolík, Gurnett, Pickett, Chum, & Cornilleau-Wehrlin, 2009 showed a similar case of changes in the propagation of chorus at Earth which they showed was a temporal variation of the regime of non-linear whistler-mode generation in the source.

An analysis of the relative phase of the electric and magnetic field given in the Supporting Information (Figures S5 and S6) show that the lower frequency band is propagating away from Jupiter's equator. Based on the measured E/cB ratio, this chorus band propagates well inside the whistler mode resonance cone, most likely close to the

Gendrin angle but quasi-parallel propagation cannot be excluded. In this case the cyclotron resonant energies would be in the 10's of keV for frequencies below 3 kHz, given $n_e \approx 100$ cm^{-3} and $f_{ce} = 12$ kHz. See Figure S7 in the Supporting Information.

Based on the phase analysis shown in Figures S5 and S6, it appears the propagation of the narrowband component is varying with time, which may be an indication of a relatively local source, perhaps near Europa. A similar argument has been used with Cluster data (Santolík et al., 2005, 2009, 2010)

One other aspect of signatures observed near Europa are impulses due to the impact of micron-sized dust grains on the spacecraft in the 50 Hz - 20 kHz electric channel. Dust impacts observed by Juno Waves at the ring plane near perijoves are discussed in Ye et al., 2020. The present paper uses the same detection algorithm based on a minimum slope threshold in the voltage waveform as used in the ring plane paper. Examples of impact waveforms are given in Figure S8. The rate of these impacts is shown in Figure 4a. Little can be said about the size of the grains from the Waves data, but it is expected that these are of the order of 1 micron in radius based on the analysis in Ye et al., 2020. These authors found characteristic sizes of grains of 1.4 microns between the ring system and Jupiter's ionosphere. Because ESW's can sometimes be confused with dust impacts, we examined each of the potential impacts within about 10 minutes of closest approach and counted the number within 30-s bins. Given the duty cycle of waveform captures (122 ms/s) we multiplied the observed rate by the inverse of this (8.2) to account for this duty cycle. This duty cycle-corrected impact rate is plotted in Figure 4a. While the number of actual impacts observed is not large, there is a clear peak near Europa. As with the electron density, this peak occurs a minute or so prior to closest approach.

We can use the relative velocity of Juno with respect to Europa of 23.6 km/s, assuming the dust cloud is gravitationally bound to the moon, and the cross-sectional area of Juno presented to the presumed inflow direction of the dust relative to the $\sim$60 m^2 area of the spacecraft (mostly solar arrays) to compute the number density of grains as a function of radial distance to Europa. The angle between the assumed dust ram direction and the normal to the spacecraft cross-section (solar panel plane) is 46°, so the effective area is approximately 43 m^2. Here, we used the duty-cycle corrected number of impacts in 200-km altitude bins. The densities are perhaps an order of magnitude below those provided by Krüger, Krivov, Sremčević, & Grün, 2003, which is probably not unreasonable given large uncertainties in the Juno grain size sensitivity and effective area. We've plotted density versus radial distance in Figure 4b and superposed a power law curve of the form $N = Cr^{-2.5}$ where N is the number density in m^{-3} and r is the radial distance scaled to a Europan radius using $R_E = 1562.6$ km. We set C to 5e-6 to roughly match the measured values. This is a simplified form of the dust distribution model of Krivov, Sremčević, Spahn, Dikarev, & Kholshevnikov, 2003 using only the assumed gravitationally bound population with a power law index of -2.5. Beyond 4 or so R_E, the observed number of impacts per altitude bin are primarily zero or one. To demonstrate this, Figure 4b shows the density assuming only one dust impact in each altitude bin, the 1-count level indicated by black dots. When the computed density is similar to this level, it implies very poor statistics and the densities should be regarded with great caution. Hence, we do not place much quantitative importance on the model shown in Figure 4b because attempted actual fits to the power-law model were unsatisfactory. Nevertheless, it is illustrative to note the variation of impacts as a function of distance from Europa when the densities are above the 1-count level since the model qualitatively reflects the computed dust density for bound dust grains.

3 Discussion

The plasma density profile obtained from the upper hybrid frequencies presented here showed that the peak density seemed to occur prior to closest approach, and more aligned with the center of the geometric wake. This is consistent with the prediction of models of the flow of magnetospheric plasma past Europa (Saur et al., 1998; Dols et al., 2016). See also the comprehensive summary of the plasma environments of Io and Europa (Bagenal & Dols, 2020). The upstream electron densities measured are similar to those measured by Galileo, with the exception of Galileo's E12 flyby that exhibited extraordinarily high plasma densities (Kurth et al., 2001).

The observations of ESW's in Europa's wake are consistent with those by Galileo (Gurnett et al., 1998; Kurth et al., 2001). These structures are the result of an electron beam instability as first shown in the context of Earth's magnetotail (Matsumoto et al., 1994). Allegrini et al., 2020 reported electron beams comprising 0.4 to 25 keV electrons on field lines connected to Europa's tail footprint. They argue that the acceleration could be due to Alfvén acceleration although there is some evidence of electrostatic acceleration in the electron energy spectrum. Further, Rabia et al., 2023 show that non-monotonic electron distributions are found in footprint tail flux tubes within $\sim 4^\circ$ of the footprint, supporting electrostatic acceleration as a source for the electron beams. Gurnett et al., 2011 reported field-aligned electron beams very near Saturn's moon Enceladus that were the source of auroral hiss. These authors did not mention electrostatic solitary waves associated with these beams because the spectrum was dominated by dust impacts from the moon's plumes. However, upon close inspection, some ESW's can be found near Enceladus as shown in Figure S9 in Supporting Information. ESW's then, are an expected phenomena in an outer planet moon's interaction with the magnetosphere.

The asymmetric occurrence of whistler-mode chorus on the Jupiter-facing side of Europa is curious. We examined the JADE (McComas et al., 2017) electron distribution function for <30 keV electrons during this time period. There appeared to be no clear feature that might be expected to be unstable to chorus. We note that Kurth et al., 2001 showed whistler mode emissions on the sub-Jovian side of Europa during Galileo's E4 flyby that had a geometry similar to Juno's in that it passed through Europa's wake. However, other Galileo flybys showed whistler-mode emissions distributed more symmetrically around Europa (see Figure 14 of Kurth et al., 2001). These waves can be linked to absorption of cyclotron resonant electrons by Europa, thus creating a temperature anisotropy, which, in turn, would be unstable for whistler mode waves in Jupiter's equatorial region. These newly generated waves would propagate approximately along the magnetic field lines back to Europa. As the linear dimension of Europa is only about 2% of its distance above the magnetic equator during the Juno flyby, the waves would likely pass through a region around the moon, consistent with these new measurements and also with previous Galileo observations. In our case, Juno is not magnetically connected to Europa, so the above described deformation of the electron distribution function is not directly observed, but an absorption of electrons was documented at Rhea (Santolík et al., 2011) using Cassini measurements, which also showed newly generated whistler mode waves below one-half f_{ce}. Intense whistler mode waves are known to both accelerate and pitch-angle scatter energetic electrons, hence, are important in the dynamics of Europa's interaction with Jupiter's magnetic field.

Dust observations by the Galileo Cosmic Dust Analyzer showed a relative peak in the existence of grains near Europa (Krüger et al., 2003). These authors suggest the source of dust near Europa is due to ejecta from micrometeoroid impacts on the moon. The Juno instrument likely has less sensitivity to sub-micron grains than the Galileo dust detector system, explaining the lower densities in the observations presented here. Further, Juno does not have the ability to discern the velocities or masses of the detected grains. However, the relative concentration of dust near Europa is consistent with the Galileo observations.

4 Conclusions

Juno passed Europa at an altitude of 355 km on 29 September 2022. As one of Juno's in situ science instruments, the Waves instrument obtained electric and magnetic plasma wave observations at frequencies up to 20 kHz and continuing to 150 kHz and above using only its electric antenna. The plasma waves are essential contributors to Europa's interaction with its environment. There was a significant separation between the Europa flyby and Juno's crossing of Jupiter's magnetic equator, enabling a unique identification of effects associated with the moon as opposed to magnetospheric phenomena normally occurring at the magnetic equator near 10 R_J. Juno observed two bands of chorus exhibiting different propagation characteristics. Given the separation of this flyby from the magnetic equator crossing, it is more clear these waves are associated with Europa than was possible to discern with Galileo. Further, we suggest these emissions are due to the asymmetric absorption of electrons by Europa, generating the emissions near Jupiter's magnetic equator below the moon. As with Galileo, a band at the upper hybrid frequency was observed providing the local plasma density. This showed a peak in the wake, not dissimilar to that observed by Galileo on its E4 flyby (Gurnett et al., 1998; Kurth et al., 2001). The plasma density measurements are essential in modeling any magnetosphere-Europa interaction observed by Juno. As was the case during Galileo wake crossings, electrostatic solitary waves were observed by Juno. These ESWs are associated with electron beams and could be related to currents connecting Europa with Jupiter's ionosphere. Juno observed impulses due to micron-sized impacts with a local maximum very close to Europa. The Galileo wave observations, in conjunction with magnetic field observations and modeling were used by Jia et al., 2018 to suggest a plume at Europa during the G12 flyby. There was no evidence of a plume in the Juno Waves observations at Europa and the upstream electron densities observed by Juno are on the low side of those observed by Galileo (Kurth et al., 2001).

Acknowledgments

The research at the University of Iowa is supported by NASA through Contract 699041X with the Southwest Research Institute. OS acknowledges support from grant LUAUS23152. WSK acknowledges the use of the Space Physics Data Repository at the University of Iowa supported by the Roy J. Carver Charitable Trust.

Open Research

The Juno Waves data used in this paper are available from the PDS at (Kurth & Piker, 2022a) and (Kurth & Piker, 2022b). The electron densities in Figures 2 and 3 are at (Kurth et al., 2023).

References From the Supporting Information

(Barbosa & Kurth, 1980) (Kurth et al., 2001) (Shen et al., 2021) (Yoon et al., 1996) (Zhang et al., 2021)

References

Allegrini, F., Ebert, R. W., Szalay, J. R., Bagenal, F., Bolton, S. J., Clark, G. B., ... Wilson, R. J. (2022, December). Overview of Plasma Observations During the Recent Europa Flyby from Juno/JADE. In *Agu fall meeting abstracts* (Vol. 2022, p. P45F-2531).

Allegrini, F., Gladstone, G. R., Hue, V., Clark, G., Szalay, J. R., Kurth, W. S., ... Wilson, R. J. (2020, September). First Report of Electron Measurements During a Europa Footprint Tail Crossing by Juno. *Geophysical Research Letters*, *47*(18), e89732. doi: 10.1029/2020GL089732

Bagenal, F., & Dols, V. (2020, May). The Space Environment of Io and Eu-

ropa. *Journal of Geophysical Research (Space Physics)*, *125*(5), e27485. doi: 10.1029/2019JA027485

Barbosa, D. D., & Kurth, W. S. (1980, December). Superthermal electrons and Bernstein waves in Jupiter's inner magnetosphere. *Journal of Geophysical Research*, *85*(A12), 6729-6742. doi: 10.1029/JA085iA12p06729

Bonfond, B., Saur, J., Grodent, D., Badman, S. V., Bisikalo, D., Shematovich, V., ... Radioti, A. (2017, August). The tails of the satellite auroral footprints at Jupiter. *Journal of Geophysical Research (Space Physics)*, *122*(8), 7985-7996. doi: 10.1002/2017JA024370

Connerney, J. E. P., Benn, M., Bjarno, J. B., Denver, T., Espley, J., Jorgensen, J. L., ... Smith, E. J. (2017, November). The Juno Magnetic Field Investigation. *Space Science Reviews*, *213*(1-4), 39-138. doi: 10.1007/s11214-017-0334-z

Dols, V. J., Bagenal, F., Cassidy, T. A., Crary, F. J., & Delamere, P. A. (2016, January). Europa's atmospheric neutral escape: Importance of symmetrical O_2 charge exchange. *Icarus*, *264*, 387-397. doi: 10.1016/j.icarus.2015.09.026

Gurnett, D. A., Averkamp, T. F., Schippers, P., Persoon, A. M., Hospodarsky, G. B., Leisner, J. S., ... Dougherty, M. K. (2011, March). Auroral hiss, electron beams and standing Alfvén wave currents near Saturn's moon Enceladus. *Geophysical Research Letters*, *38*(6), L06102. doi: 10.1029/2011GL046854

Gurnett, D. A., & Bhattacharjee, A. (2017). *Introduction to Plasma Physics*.

Gurnett, D. A., Kurth, W. S., Roux, A., Bolton, S. J., Thomsen, E. A., & Groene, J. B. (1998, February). Galileo plasma wave observations near Europa. *Geophysical Research Letters*, *25*(3), 237-240. doi: 10.1029/97GL03706

Jia, X., Kivelson, M. G., Khurana, K. K., & Kurth, W. S. (2018, May). Evidence of a plume on Europa from Galileo magnetic and plasma wave signatures. *Nature Astronomy*, *2*, 459-464. doi: 10.1038/s41550-018-0450-z

Joy, S. P., & Mafi, J. N. (2002). *GO JUP POS GLL TRAJECTORY MOON CENTERED COORDS V1.0, GO-J-POS-6-SC-TRAJ-MOON-COORDS-V1.0 [Dataset]*. NASA Planetary Data System. doi: 10.17189/1519677

Khurana, K. K., Kivelson, M. G., Stevenson, D. J., Schubert, G., Russell, C. T., Walker, R. J., & Polanskey, C. (1998, October). Induced magnetic fields as evidence for subsurface oceans in Europa and Callisto. *Nature*, *395*(6704), 777-780. doi: 10.1038/27394

Kivelson, M. G., Khurana, K. K., Means, J. D., Russell, C. T., & Snare, R. C. (1992, May). The Galileo magnetic field investigation. *Space Science Reviews*, *60*(1-4), 357-383. doi: 10.1007/BF00216862

Kivelson, M. G., Khurana, K. K., Russell, C. T., Volwerk, M., Walker, R. J., & Zimmer, C. (2000, August). Galileo Magnetometer Measurements: A Stronger Case for a Subsurface Ocean at Europa. *Science*, *289*(5483), 1340-1343. doi: 10.1126/science.289.5483.1340

Kolmašová, I., Imai, M., Santolík, O., Kurth, W. S., Hospodarsky, G. B., Gurnett, D. A., ... Bolton, S. J. (2018, June). Discovery of rapid whistlers close to Jupiter implying lightning rates similar to those on Earth. *Nature Astronomy*, *2*, 544-548. doi: 10.1038/s41550-018-0442-z

Krivov, A. V., Sremčević, M., Spahn, F., Dikarev, V. V., & Kholshevnikov, K. V. (2003, March). Impact-generated dust clouds around planetary satellites: spherically symmetric case. *Planetary and Space Science*, *51*(3), 251-269. doi: 10.1016/S0032-0633(02)00147-2

Krüger, H., Krivov, A. V., Sremčević, M., & Grün, E. (2003, July). Impact-generated dust clouds surrounding the Galilean moons. *Icarus*, *164*(1), 170-187. doi: 10.1016/S0019-1035(03)00127-1

Kurth, W. S., Gurnett, D. A., Persoon, A. M., Roux, A., Bolton, S. J., & Alexander, C. J. (2001, March). The plasma wave environment of Europa. *Planetary and Space Science*, *49*(3-4), 345-363. doi: 10.1016/S0032-0633(00)00156-2

Kurth, W. S., Hospodarsky, G. B., Kirchner, D. L., Mokrzycki, B. T., Averkamp, T. F., Robison, W. T., ... Zarka, P. (2017, November). The Juno Waves Investigation. *Space Science Reviews*, *213*, 347-392. doi: 10.1007/s11214-017-0396-y

Kurth, W. S., & Piker, C. W. (2022a). *Juno e/j/s/ss waves calibrated burst full resolution v2.0, jno-e/j/ss-wav-3-cdr-bstfull-v2.0* [dataset]. NASA Planetary Data System. doi: 10.17189/1522461

Kurth, W. S., & Piker, C. W. (2022b). *JUNO E/J/S/SS WAVES CALIBRATED SURVEY FULL RESOLUTION V2.0, JNO-E/J/SS-WAV-3-CDR-SRVFULL-V2.0* [dataset]. NASA Planetary Data System. doi: 10.17189/1520498

Kurth, W. S., Wilkinson, D. R., Hospodarsky, G. B., Santolík, O., Averkamp, T. F., Sulaiman, A. H., ... Bolton, S. J. (2023). *Juno Plasma Wave Observations at Europa (1.0.0)* [dataset]. Zenodo. doi: 10.5281/zenodo.10215629

Matsumoto, H., Kojima, H., Miyatake, T., Omura, Y., Okada, M., Nagano, I., & Tsutsui, M. (1994, December). Electrostatic solitary waves (ESW) in the magnetotail: BEN wave forms observed by GEOTAIL. *Geophysical Research Letters*, *21*(25), 2915-2918. doi: 10.1029/94GL01284

McComas, D. J., Alexander, N., Allegrini, F., Bagenal, F., Beebe, C., Clark, G., ... White, D. (2017, November). The Jovian Auroral Distributions Experiment (JADE) on the Juno Mission to Jupiter. *Space Science Reviews*, *213*(1-4), 547-643. doi: 10.1007/s11214-013-9990-9

Moirano, A., Mura, A., Adriani, A., Dols, V., Bonfond, B., Waite, J. H., ... Bolton, S. J. (2021, September). Morphology of the Auroral Tail of Io, Europa, and Ganymede From JIRAM L-Band Imager. *Journal of Geophysical Research (Space Physics)*, *126*(9), e29450. doi: 10.1029/2021JA029450

Mosier, S. R., & Gurnett, D. A. (1971, February). Theory of the Injun 5 very-low-frequency Poynting flux measurements. *Journal of Geophysical Research*, *76*(4), 972-977. doi: 10.1029/JA076i004p00972

Pappalardo, R. T., Vance, S., Bagenal, F., Bills, B. G., Blaney, D. L., Blankenship, D. D., ... Soderlund, K. M. (2013, August). Science Potential from a Europa Lander. *Astrobiology*, *13*(8), 740-773. doi: 10.1089/ast.2013.1003

Rabia, J., Hue, V., Szalay, J. R., André, N., Nénon, Q., Blanc, M., ... Sulaiman, A. H. (2023). Evidence for non-monotonic and broadband electron distributions in the europa footprint tail revealed by juno in situ measurements. *Geophysical Research Letters*, *50*(12), e2023GL103131. Retrieved from `https://agupubs.onlinelibrary.wiley.com/doi/abs/10.1029/2023GL103131` (e2023GL103131 2023GL103131) doi: https://doi.org/10.1029/2023GL103131

Roth, L., Saur, J., Retherford, K. D., Strobel, D. F., Feldman, P. D., McGrath, M. A., & Nimmo, F. (2014, January). Transient Water Vapor at Europa's South Pole. *Science*, *343*(6167), 171-174. doi: 10.1126/science.1247051

Santolík, O., Gurnett, D. A., Jones, G. H., Schippers, P., Crary, F. J., Leisner, J. S., ... Dougherty, M. K. (2011, October). Intense plasma wave emissions associated with Saturn's moon Rhea. *Geophysical Research Letters*, *38*(19), L19204. doi: 10.1029/2011GL049219

Santolík, O., Gurnett, D. A., Pickett, J. S., Chum, J., & Cornilleau-Wehrlin, N. (2009, December). Oblique propagation of whistler mode waves in the chorus source region. *Journal of Geophysical Research (Space Physics)*, *114*(A12), A00F03. doi: 10.1029/2009JA014586

Santolík, O., Gurnett, D. A., Pickett, J. S., Grimald, S., Décreau, P. M. E., Parrot, M., ... Fazakerley, A. (2010, August). Wave-particle interactions in the equatorial source region of whistler-mode emissions. *Journal of Geophysical Research (Space Physics)*, *115*(15), A00F16. doi: 10.1029/2009JA015218

Santolík, O., Gurnett, D. A., Pickett, J. S., Parrot, M., & Cornilleau-Wehrlin, N. (2005, January). Central position of the source region of storm-time chorus. *Planetary and Space Science*, *53*(1-3), 299-305. doi: 10.1016/j.pss.2004.09.056

Saur, J., Strobel, D. F., & Neubauer, F. M. (1998, September). Interaction of the Jovian magnetosphere with Europa: Constraints on the neutral atmosphere. *Journal of Geophysical Research*, *103*(E9), 19947-19962. doi: 10.1029/97JE03556

Shen, M. M., Sternovsky, Z., Horányi, M., Hsu, H.-W., & Malaspina, D. M. (2021, April). Laboratory Study of Antenna Signals Generated by Dust Impacts on Spacecraft. *Journal of Geophysical Research (Space Physics)*, *126*(4), e28965. doi: 10.1029/2020JA028965

Sparks, W. B., Schmidt, B. E., McGrath, M. A., Hand, K. P., Spencer, J. R., Cracraft, M., & E Deustua, S. (2017, April). Active Cryovolcanism on Europa? *Astrophysical Journal Letters*, *839*(2), L18. doi: 10.3847/2041-8213/aa67f8

Volwerk, M., Khurana, K., & Kivelson, M. (2007, May). Europa's Alfvén wing: shrinkage and displacement influenced by an induced magnetic field. *Annales Geophysicae*, *25*(4), 905-914. doi: 10.5194/angeo-25-905-2007

Ye, S. Y., Averkamp, T. F., Kurth, W. S., Brennan, M., Bolton, S., Connerney, J. E. P., & Joergensen, J. L. (2020, June). Juno Waves Detection of Dust Impacts Near Jupiter. *Journal of Geophysical Research (Planets)*, *125*(6), e06367. doi: 10.1029/2019JE006367

Yoon, P. H., Weatherwax, A. T., Rosenberg, T. J., & LaBelle, J. (1996, December). Lower ionospheric cyclotron maser theory: A possible source of $2f_{ce}$ and $3f_{ce}$ auroral radio emissions. *Journal of Geophysical Research*, *101*(A12), 27015-27026. doi: 10.1029/96JA02664

Zhang, X., Angelopoulos, V., Artemyev, A. V., Zhang, X.-J., & Liu, J. (2021, March). Beam Driven Electron Cyclotron Harmonic Waves in Earth's Magnetotail. *Journal of Geophysical Research (Space Physics)*, *126*(3), e28743. doi: 10.1029/2020JA028743

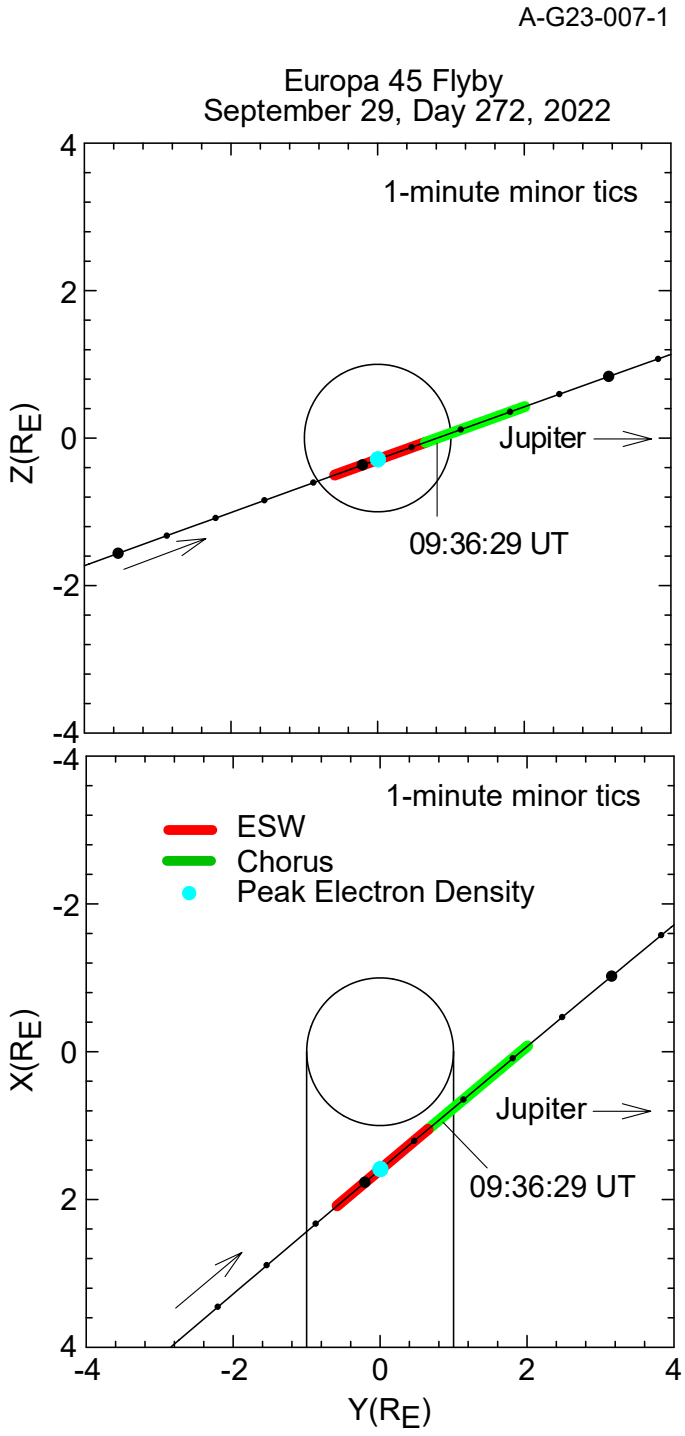

Figure 1. The geometry of the Juno Europa flyby projected into the Y-X and Y-Z planes using EPhiO coordinates described in the text. Distances are in units of Europa radii (R_E = 1562.6 km). The red-highlighted segment represents times when electrostatic solitary waves were detected. The green segment indicates when chorus was detected. The cyan dot is the time Waves detected the maximum electron density at ~330 cm^{-3}.

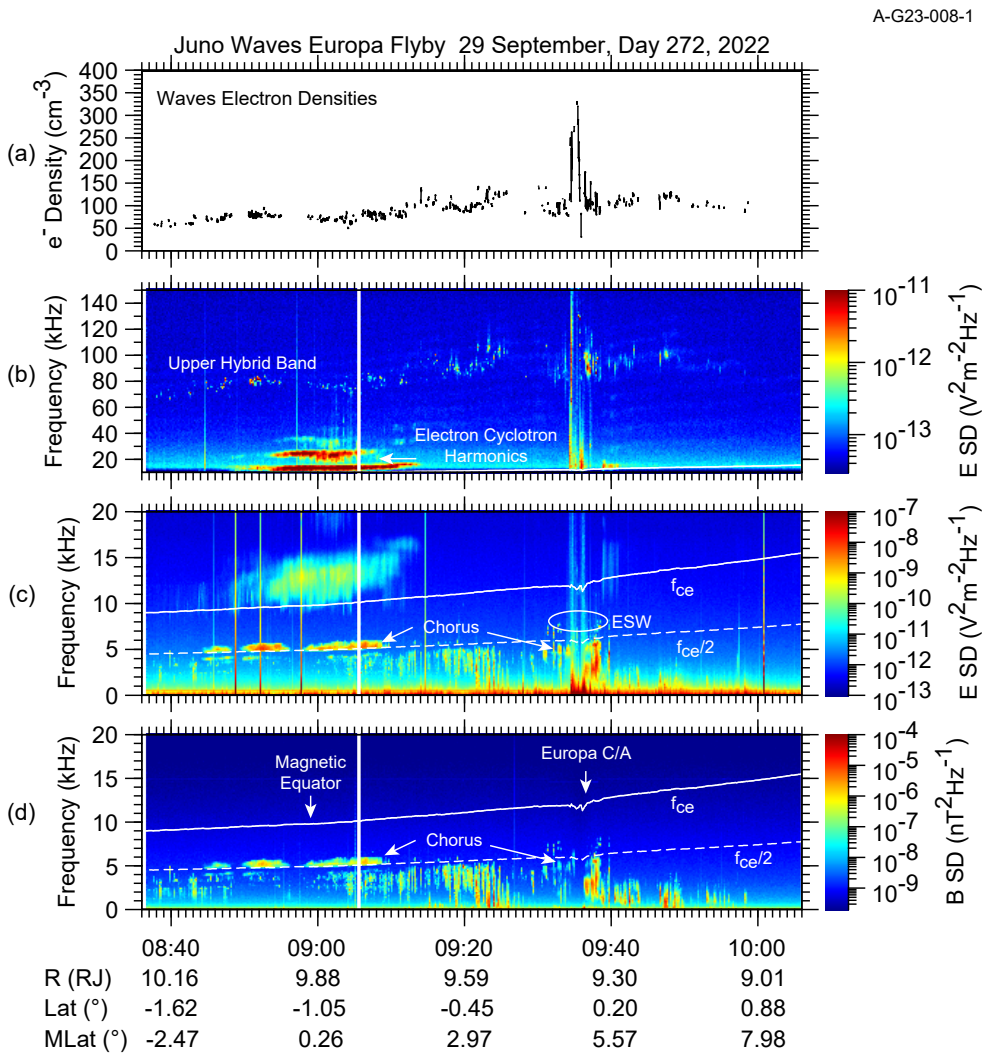

Figure 2. A summary of plasma wave observations near the Europa flyby, but extending earlier in time to include the crossing of the magnetic equator which is the site of several plasma wave phenomena. This display shows the separation of the flyby from the magnetic equator crossing, hence, allows for the separation of phenomena related to Europa from normal magnetospheric phenomena. (a) Electron density from the upper hybrid emissions shown in panel b. (b) Electric field spectrogram from 10 to 150 kHz showing upper hybrid emissions from $\sim$ 50 to above 100 kHz. (c) Electric field spectrogram from 50 Hz to 20 kHz. (d) Magnetic field spectrogram from 50 Hz to 20 kHz. The solid white line is at the electron cyclotron frequency. The dashed line denotes $f_{ce}/2$. R_J refers to Jovian radii.

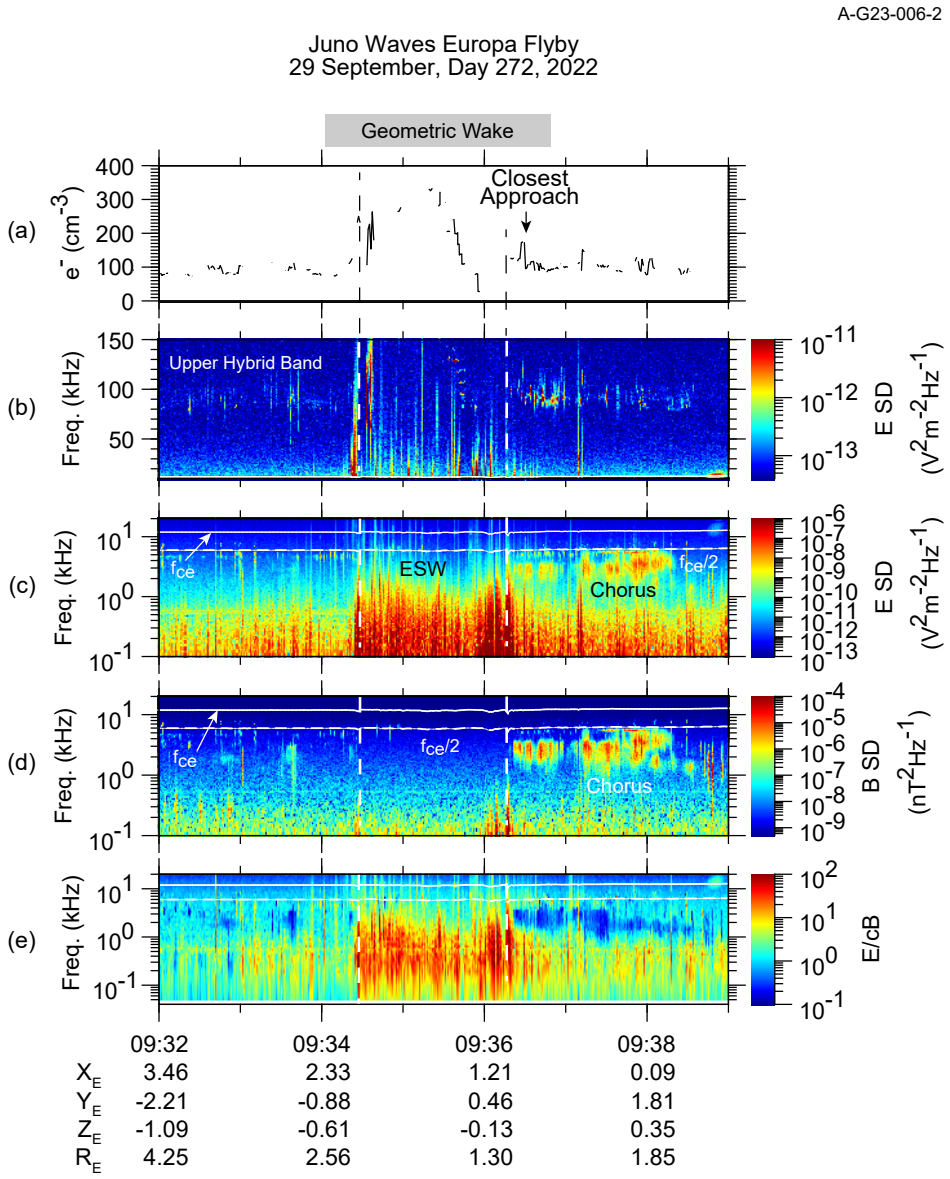

Figure 3. A display similar in format to Figure 2, expanding the time around Europa closest approach and using a logarithmic frequency axis for the waves below 20 kHz. (e) The ratio of E/cB is included to aid in the identification of electrostatic emissions with $E/cB \gg 1$ and electromagnetic waves with E/cB closer to 1. The gray bar at the top indicates the time during which Juno was within the geometric wake of Europa. The vertical dashed lines indicate times when JADE observed field-aligned electron beams and a dropout of magnetospheric energetic electrons.

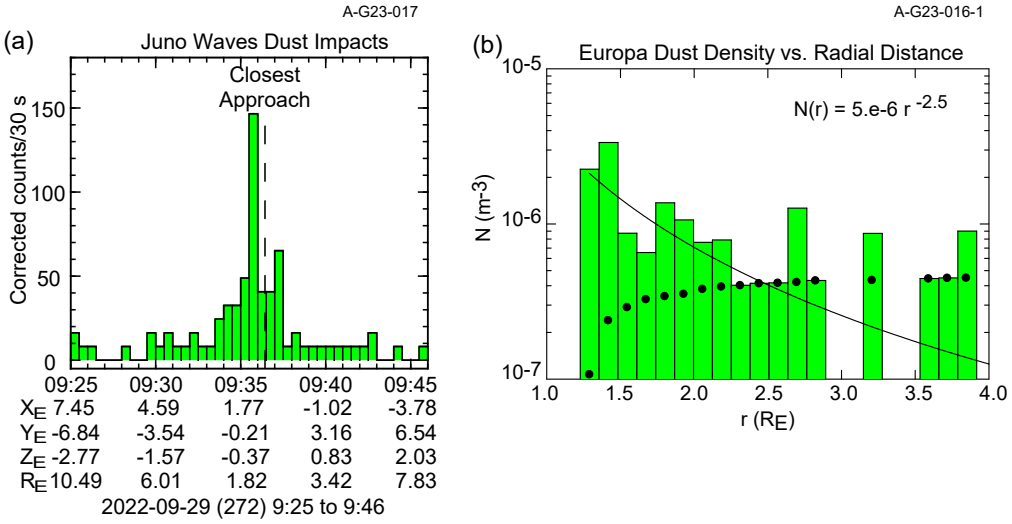

Figure 4. (a) The duty cycle-corrected rate of impacts detected within about 10 minutes of the closest approach to Europa. (b) The estimated dust density as a function of radial distance to Europa r (R_E) in 200-km altitude bins shown in histogram form. Dots indicate the 1-count level (see text). Superposed on this plot is a representative model, not a fit, of bound dust near Europa (see text).